

# Adaptive multilevel iterative techniques for nonconforming finite element discretizations

R.H.W. HOPPE and B. WOHLMUTH<sup>1</sup>

**Abstract** — We consider adaptive multilevel methods for the nonconforming P1 finite element approximation of linear second order elliptic boundary value problems. Emphasis is on the efficient solution of the discretized problems by multilevel preconditioned conjugate gradient iterations with respect to an adaptively generated hierarchy of possibly highly nonuniform triangulations. Local refinement of the elements of the triangulations is done by means of an efficient and reliable element-oriented a posteriori error estimator that can be derived by a defect correction in a higher order ansatz space and its hierarchical two-level splitting. The performance of the preconditioners and the error estimator is illustrated by some test examples. Further, numerical results are given for the reverse biased  $pn$ -junction in semiconductor device simulation and the two-group diffusion equations modeling the neutron fluxes in nuclear reactors.

**Keywords:** nonconforming finite elements, multilevel preconditioners, adaptive grid refinement

**AMS(MOS) subject classification.** 65F10, 65N30, 65N50, 65N55.

## 1. INTRODUCTION

In recent years there has been a considerable interest in the construction and implementation of multilevel methods for the iterative solution of linear second order elliptic boundary value problems discretized by the lowest order Crouzeix-Raviart elements. As far as the application of classical multigrid methods with respect to a hierarchy of uniformly refined simplicial triangulations is concerned, we refer to the pioneering work done by Braess and Verfürth [9] and by Brenner [11]. In the context of multilevel preconditioned conjugate gradient iterations, substantial developments have been achieved by Oswald who considered both a hierarchical basis multilevel method [25] and a multilevel preconditioner of BPX-type [27] (cf. also Oswald's monograph [28] and Zhang's survey article [39]). We refer to the authors' article [35] for a comparison of these preconditioners. However, for nonconforming discretizations less work has been done concerning the realization of adaptive grid refinement based on appropriate a posteriori error estimators. In particular, in [18] the authors have developed both edge-oriented and element-oriented a posteriori error estimators using the well-known principle of defect correction in a higher order ansatz space adapted to the nonconforming setting.

In this paper, we shall be concerned with the construction and implementation of both a hierarchical and a BPX-type preconditioner that can be obtained by taking advantage of techniques due to Cowsar [13] in the framework of domain decomposition methods (for

---

<sup>1</sup>Math. Institute, University of Augsburg, D-86135 Augsburg, Germany.  
E-mail: hoppe@math.uni-augsburg.de, wohlmuth@math.uni-augsburg.de

similar ideas cf. also Sarkis [29]). The multilevel iterative solution process will go hand in hand with an adaptive grid refinement technique relying on the element-oriented error estimator developed by the authors in [18].

We consider the following boundary value problem for a linear second order elliptic differential operator

$$\begin{aligned} Lu := -\operatorname{div}(a\nabla u) + bu &= f & \text{in } \Omega, \\ u &= 0 & \text{on } \Gamma := \partial\Omega \end{aligned} \quad (1.1)$$

where  $\Omega$  stands for a bounded, polygonal domain in the Euclidean space  $\mathbb{R}^2$  and  $f \in L^2(\Omega)$ . Furthermore, we assume  $a = (a_{ij})_{i,j=1}^2$  to be a symmetric, matrix-valued function with  $a_{ij} \in L^\infty(\Omega)$ ,  $1 \leq i, j \leq 2$ , and  $b \in L^\infty(\Omega)$  satisfying

$$\begin{aligned} \alpha_0 |\xi|^2 \leq \sum_{i,j=1}^2 a_{ij}(x) \xi_i \xi_j \leq \alpha_1 |\xi|^2, \quad \xi \in \mathbb{R}^2, \quad 0 < \alpha_0 \leq \alpha_1, \\ 0 \leq b_0 \leq b(x) \leq b_1 \end{aligned} \quad (1.2)$$

for almost all  $x \in \Omega$ . We note that only for simplicity we have chosen homogeneous Dirichlet boundary data. All subsequent results carry over to more general boundary conditions without major difficulties.

Denoting by  $a(\cdot, \cdot)$  the bilinear form on  $H_0^1(\Omega) \times H_0^1(\Omega)$  given by

$$a(u, v) := \int_{\Omega} (a\nabla u \cdot \nabla v + buv) dx, \quad u, v \in H_0^1(\Omega),$$

the variational formulation of (1.1) is to find  $u \in H_0^1(\Omega)$  such that

$$a(u, v) = (f, v)_{0;\Omega}, \quad v \in H_0^1(\Omega) \quad (1.3)$$

where  $(\cdot, \cdot)_{0;\Omega}$  stands for the standard inner product on  $L^2(\Omega)$ .

In the sequel, for  $D \subset \Omega$  we refer to  $\|\cdot\|_{0;D}$  as the standard  $L^2$ -norm whereas  $|\cdot|_{1;D}$  and  $\|\cdot\|_{1;D}$  stand for the  $H^1$ -seminorm and  $H^1$ -norm, respectively. Finally, we mention the well-known Poincaré-Friedrichs inequality

$$\|v\|_{0;\Omega}^2 \leq C_P |v|_{1;\Omega}^2, \quad v \in H_0^1(\Omega). \quad (1.4)$$

Concerning the nonconforming P1 approximation of (1.1), we assume that  $(\mathcal{T}_k)_{k=0}^j$ ,  $j \in \mathbb{N}$ , is a hierarchy of simplicial triangulations of  $\Omega$  generated by the refinement process due to Bank et al. (cf. e.g. [3], [4]). For  $k \geq 0$  we denote by  $\mathcal{E}_k$  the set of the edges of  $\mathcal{T}_k$ , by  $\mathcal{M}_k$  the set of the midpoints of the edges and by  $\mathcal{N}_k$  the set of the vertices of the elements. We set  $\mathcal{L}_k^0 := \mathcal{L}_k \cap \Omega$  and  $\mathcal{L}_k^\Gamma := \mathcal{L}_k \cap \Gamma$  where  $\mathcal{L}_k \in \{\mathcal{E}_k, \mathcal{M}_k, \mathcal{N}_k\}$ . Further, for  $T \in \mathcal{T}_k$ ,  $k \geq 0$ , we refer to  $P_l(T)$ ,  $l \in \mathbb{N}$ , as the linear space of polynomials of degree  $\leq l$  on  $T$ , to  $h_T$  as the diameter of  $T$  and to  $m_i$  and  $p_i$ ,  $1 \leq i \leq 3$ , as the midpoints of the edges of  $T$  and the vertices of  $T$ , respectively. Moreover, for  $p \in \mathcal{N}_k$ ,  $k \geq 0$ , we denote by  $D_p$  the set of all adjacent elements, i.e., the set of all  $T \in \mathcal{T}_k$  having  $p$  as a common vertex.

As a consequence of the refinement process the triangulations  $\mathcal{T}_k$ ,  $k \geq 0$ , are locally quasiuniform, i.e., there exists a constant  $\kappa_0 > 0$  depending only on the local geometry of the initial triangulation  $\mathcal{T}_0$  such that

$$\frac{h_T}{h_{T'}} \leq \kappa_0 \quad (1.5)$$

for all  $T, T' \in \mathcal{T}_k$  with  $T \cap T' \neq \emptyset$ . Moreover, there exists a further constant  $\kappa_1$  depending only on the local geometry of  $\mathcal{T}_0$  such that for all  $p \in \mathcal{N}_k$ ,  $k \geq 0$

$$\text{card}D_p \leq \kappa_1. \quad (1.6)$$

Finally, in the sequel we will take advantage of the following norm equivalences: There exist constants  $0 < c_\nu \leq C_\nu$ ,  $0 \leq \nu \leq 1$ , depending only on the local geometry of  $\mathcal{T}_0$  such that for all  $v \in P_1(T)$ ,  $T \in \mathcal{T}_k$ ,  $k \geq 0$

$$\begin{aligned} c_0 h_T^2 \sum_{i=1}^3 v^2(q_i) &\leq \|v\|_{0;T}^2 \leq C_0 h_T^2 \sum_{i=1}^3 v^2(q_i), \\ c_1 \sum_{\substack{i,j=1 \\ i < j}}^3 (v(q_i) - v(q_j))^2 &\leq |v|_{1;T}^2 \leq C_1 \sum_{\substack{i,j=1 \\ i < j}}^3 (v(q_i) - v(q_j))^2 \end{aligned} \quad (1.7)$$

where either  $q_i = p_i$  or  $q_i = m_i$ ,  $1 \leq i \leq 3$ .

After these prerequisites we refer to

$$\begin{aligned} CR_{1,0}(\Omega; \mathcal{T}_k) &:= \{v_k \in L^2(\Omega) \mid v_k|_T \in P_1(T), T \in \mathcal{T}_k, \\ &\quad v_k|_T(m) = v_k|_{T'}(m), m \in (T \cap T') \cap \mathcal{M}_k^0, v_k(m) = 0, m \in \mathcal{M}_k^\Gamma\} \end{aligned}$$

as the lowest order nonconforming Crouzeix-Raviart finite element space (cf. e.g. [12]). We further define  $a_{CR}(\cdot, \cdot)$  as the bilinear form on  $CR_{1,0}(\Omega; \mathcal{T}_k) \times CR_{1,0}(\Omega; \mathcal{T}_k)$  given by

$$\begin{aligned} a_{CR}(u_k, v_k) &:= \sum_{T \in \mathcal{T}_k} a_{CR}|_T(u_k, v_k), \quad u_k, v_k \in CR_{1,0}(\Omega; \mathcal{T}_k), \\ a_{CR}|_T(u_k, v_k) &:= \int_T (a \nabla u_k \cdot \nabla v_k + b u_k v_k) dx, \quad u_k, v_k \in CR_{1,0}(\Omega; \mathcal{T}_k). \end{aligned}$$

Then, the nonconforming P1 approximation of (1.1) with respect to the finest triangulation  $\mathcal{T}_j$  amounts to the computation of  $u_j \in CR_{1,0}(\Omega; \mathcal{T}_j)$  such that

$$a_{CR}(u_j, v_j) = (f, v_j)_{0;\Omega}, \quad v_j \in CR_{1,0}(\Omega; \mathcal{T}_j). \quad (1.8)$$

We note that under the assumptions (1.2) there exists a unique solution to (1.8). Moreover, if the solution  $u \in H_0^1(\Omega)$  of (1.3) satisfies  $u \in H^2(\Omega)$ , then  $u_j$  approximates  $u$  of order  $O(h)$ ,  $h := \max_{T \in \mathcal{T}_j} h_T$ , with respect to the energy norm  $\|\cdot\|_j := a_{CR}(\cdot, \cdot)^{1/2}$  (cf. e.g. [12]).

In the following section, (1.8) will be solved by preconditioned conjugate gradient methods constructed with respect to an associated hierarchy of conforming finite element spaces. For that purpose we refer to

$$S_{1,0}(\Omega; \mathcal{T}_k) := \{v_k \in C_0(\Omega) \mid v_k|_T \in P_1(T), T \in \mathcal{T}_k\}$$

as the standard conforming finite element space of continuous, piecewise linear functions vanishing on the boundary  $\Gamma = \partial\Omega$ .

## 2. THE MULTILEVEL PRECONDITIONERS

It is well known that in case of the standard conforming P1 approximation of linear second order elliptic boundary value problems both Yserentant's hierarchical basis preconditioner [37] and the BPX-preconditioner are based on the fact that the hierarchy of finite element spaces  $S_{1,0}(\Omega; \mathcal{T}_k)$ ,  $1 \leq k \leq j$ , represents a nested sequence of subspaces of  $H_0^1(\Omega)$ . This

property does not hold true in the nonconforming setting. In fact, the non-nestedness of the sequence of Crouzeix-Raviart spaces  $CR_{1,0}(\Omega; \mathcal{T}_k)$ ,  $1 \leq k \leq j$ , constitutes an inherent difficulty for the development of appropriate multilevel preconditioners. A convenient remedy to overcome this problem is to embed the nonconforming ansatz space  $CR_{1,0}(\Omega; \mathcal{T}_j)$  into an appropriate conforming finite element space and to construct a multilevel preconditioner based on the associated hierarchy of conforming ansatz spaces (cf. e.g. [27, 28]). In this paper, we will follow the same approach. However, in contrast to the technique presented in [27], we will use an embedding that has been proposed by Cowsar [13] in the context of domain decomposition methods for nonconforming P1 approximations.

We consider a fictitious triangulation  $\mathcal{T}_{j+1}$  obtained from  $\mathcal{T}_j$  by uniform refinement. Obviously, the midpoints of the edges of  $\mathcal{T}_j$  turn out to be vertices of  $\mathcal{T}_{j+1}$  and consequently, the nodal points with respect to  $CR_{1,0}(\Omega; \mathcal{T}_j)$  represent a subset of the nodal points of  $S_{1,0}(\Omega; \mathcal{T}_{j+1})$ . Following [13], we introduce a pseudo-interpolation operator  $P_{CR} : CR_{1,0}(\Omega; \mathcal{T}_j) \rightarrow S_{1,0}(\Omega; \mathcal{T}_{j+1})$  which is defined by means of its values in interior vertices  $p$  of  $\mathcal{T}_{j+1}$ :

$$(P_{CR}v_j)(p) := \begin{cases} v_j(p), & p \in \mathcal{M}_j^0 \subset \mathcal{N}_{j+1}^0 \\ \frac{1}{\nu_p} \sum_{\nu=1}^{\nu_p} v_j(m_\nu^p), & p \in \mathcal{N}_{j+1}^0 \setminus \mathcal{M}_j^0. \end{cases} \quad (2.1)$$

Here,  $m_\nu^p \in \mathcal{M}_j^0$ ,  $1 \leq \nu \leq \nu_p$ , denote the midpoints of those edges in  $\mathcal{E}_j^0$  containing the interior vertex  $p \in \mathcal{N}_{j+1}^0 \setminus \mathcal{M}_j^0$ .

**Lemma 2.1.** (cf. [13; Thm. 2.1]). *Let  $P_{CR}$  be the linear mapping given by (2.1). Then there exist constants  $0 < \gamma_{CR} \leq \Gamma_{CR}$  depending only on  $\alpha_i, b_i$ ,  $0 \leq i \leq 1$ , from (1.2) and on the local geometry of  $\mathcal{T}_0$  such that for all  $v_j \in CR_{1,0}(\Omega; \mathcal{T}_j)$*

$$\gamma_{CR} a_{CR}(v_j, v_j) \leq a(P_{CR}v_j, P_{CR}v_j) \leq \Gamma_{CR} a_{CR}(v_j, v_j). \quad (2.2)$$

**Proof:** In view of (1.2) and (1.7) it is sufficient to prove the existence of constants  $0 < \gamma_i \leq \Gamma_i$ ,  $0 \leq i \leq 1$ , depending only on the local geometry of  $\mathcal{T}_0$  such that

$$\gamma_0 \sum_{T \in \mathcal{T}_j} h_T^2 \sum_{i=1}^3 v_j^2(m_i) \leq \sum_{T \in \mathcal{T}_{j+1}} \sum_{i=1}^3 (P_{CR}v_j)^2(p_i) \leq \Gamma_0 \sum_{T \in \mathcal{T}_j} h_T^2 \sum_{i=1}^3 v_j^2(m_i) \quad (2.3)$$

$$\begin{aligned} \gamma_1 \sum_{T \in \mathcal{T}_j} h_T^2 \sum_{\substack{k,l=1 \\ k < l}}^3 (v_j(m_k) - v_j(m_l))^2 &\leq \sum_{T \in \mathcal{T}_{j+1}} \sum_{\substack{k,l=1 \\ k < l}}^3 (P_{CR}v_j(p_k) - P_{CR}v_j(p_l))^2 \\ \sum_{T \in \mathcal{T}_{j+1}} \sum_{\substack{k,l=1 \\ k < l}}^3 (P_{CR}v_j(p_k) - P_{CR}v_j(p_l))^2 &\leq \Gamma_1 \sum_{T \in \mathcal{T}_j} h_T^2 \sum_{\substack{k,l=1 \\ k < l}}^3 (v_j(m_k) - v_j(m_l))^2. \end{aligned} \quad (2.4)$$

Since  $\mathcal{M}_j^0 \subset \mathcal{N}_{j+1}^0$  and  $(P_{CR}v_j)(p) = v_j(p)$ ,  $p \in \mathcal{M}_j^0$ , the lower bounds in (2.3) and (2.4) are readily established. For the proof of the upper bound in (2.3) let  $T \in \mathcal{T}_{j+1}$  and  $p \in \mathcal{N}_{j+1}^0 \cap \partial T$ . Observing (2.1), we only have to consider the case  $p \in \mathcal{N}_{j+1}^0 \setminus \mathcal{M}_j^0$ . By the Cauchy-Schwarz inequality it follows that

$$h_T^2 (P_{CR}v_j)^2(p) \leq \frac{1}{\nu_p} h_T^2 \sum_{\nu=1}^{\nu_p} v_j^2(m_\nu^p).$$

Taking into account the local quasiuniformity (1.5) of  $\mathcal{T}_j$  and  $\nu_p \leq \kappa_1$  which is a consequence of (1.6), we conclude by summing over all triangles  $T \in \mathcal{T}_{j+1}$ . The proof of the upper bound in (2.4) follows the same line of arguments.  $\square$

By means of the previous result we may identify  $P_{CR}CR_{1,0}(\Omega; \mathcal{T}_k)$  with a closed subspace of  $S_{1,0}(\Omega; \mathcal{T}_{j+1})$ . This enables us to use appropriate multilevel preconditioners with respect to the hierarchy of nested conforming ansatz spaces  $S_{1,0}(\Omega; \mathcal{T}_k)$ ,  $0 \leq k \leq j+1$ . In particular, we consider both Yserentant's hierarchical basis preconditioner  $C_{HB}$  and the BPX-preconditioner  $C_{BPX}$  (for a detailed discussion of these preconditioners cf. e.g. [6], [8], [10], [14], [36], [37]). Since we want to apply the preconditioners in the framework of the nonconforming P1 approximation, we define  $I_S : S_{1,0}(\Omega; \mathcal{T}_{j+1}) \rightarrow CR_{1,0}(\Omega; \mathcal{T}_j)$  as the pseudo-inverse of  $P_{CR}$  by  $(I_S v_{j+1})(m) := v_{j+1}(m)$ ,  $m \in \mathcal{M}_j^0$ . We then obtain the desired 'nonconforming' preconditioners  $N_{HB}$  and  $N_{BPX}$  by setting

$$N_{HB}^{-1} := I_S C_{HB}^{-1} I_S^*, \quad N_{BPX}^{-1} := I_S C_{BPX}^{-1} I_S^* \quad (2.5)$$

where  $I_S^*$  stands for the adjoint of  $I_S$ .

We note that in algebraic terms the operator  $I_S$  represents a rectangular matrix of the form  $(\text{Id}, 0)$ . Consequently, the evaluation of  $I_S^* v_j$ ,  $v_j \in CR_{1,0}(\Omega; \mathcal{T}_j)$ , does not require additional arithmetical operations. Altogether, the computational complexity is the same as in the conforming case except that we are dealing with the additional level  $j+1$ . As far as spectral condition number estimates of the preconditioned stiffness matrix are concerned, the special construction of the preconditioners  $N_{HB}$  and  $N_{BPX}$  enables us to take advantage of the corresponding results in case of the standard conforming P1 approximation. In particular, denoting by  $A_L$  the stiffness matrix associated with the conforming P1 approximation of (1.3) with respect to  $S_{1,0}(\Omega; \mathcal{T}_{j+1})$ , there exist constants  $0 < \lambda_{HB} \leq \Lambda_{HB}$  and  $0 < \lambda_{BPX} \leq \Lambda_{BPX}$  depending only on  $\alpha_i$ ,  $b_i$ ,  $0 \leq i \leq 1$ , in (1.2) and on the local geometry of  $\mathcal{T}_0$  such that for all  $v \in S_{1,0}(\Omega; \mathcal{T}_{j+1})$

$$\begin{aligned} \frac{\lambda_{HB}}{(j+2)^2} a(v, v) &\leq a(C_{HB}^{-1} A_L v, v) \leq \Lambda_{HB} a(v, v), \\ \lambda_{BPX} a(v, v) &\leq a(C_{BPX}^{-1} A_L v, v) \leq \Lambda_{BPX} a(v, v). \end{aligned} \quad (2.6)$$

The condition number estimates (2.6) have been established by various authors (cf. e.g. [8], [14], [15], [24, 26, 28], [36], [37], [38], [39]). For the proof one may either rely on the Dryja-Widlund theory of additive Schwarz methods [16] or one may use Nepomnyaschikh's fictitious domain lemma [22, 23] as has been done by Oswald in [24]. In the nonconforming setting under consideration, analogous estimates can be easily derived by means of the following abstract version of the fictitious domain lemma.

**Lemma 2.2.** *Given two Hilbert spaces  $S$ ,  $V$  with inner products  $(\cdot, \cdot)_S$  and  $(\cdot, \cdot)_V$ , let  $a_S : S \times S \rightarrow \mathbb{R}$  and  $a_V : V \times V \rightarrow \mathbb{R}$  be symmetric, positive definite bilinear forms with associated operators  $A_S : S \rightarrow S$  and  $A_V : V \rightarrow V$ . Assume that there exist a linear operator  $R : V \rightarrow S$ , an operator  $T : S \rightarrow V$  and constants  $0 < c_0 \leq c_1$  such that*

$$RTv = v, \quad v \in S, \quad (2.7 \text{ a})$$

$$c_0 a_V(Tv, Tv) \leq a_S(v, v), \quad v \in S, \quad (2.7 \text{ b})$$

$$a_S(Rv, Rv) \leq c_1 a_V(v, v), \quad v \in V. \quad (2.7 \text{ c})$$

Then there holds

$$c_0 a_S(v, v) \leq a_S(RA_V^{-1}R^*A_S v, v) \leq c_1 a_S(v, v) \quad (2.8)$$

where  $R^* : S \longrightarrow V$  denotes the adjoint of  $R$  given by means of  $(Rv, w)_S = (v, R^*w)_V$ ,  $v \in V, w \in S$ .

**Proof:** cf. e.g. [23]. □

Now, if we specify the Hilbert spaces  $S, V$ , the bilinear forms  $a_S, a_V$  and the operators  $R, T$  according to the nonconforming setting and use (2.6), we are able to prove the following spectral condition number estimates:

**Theorem 2.1.** *Let  $N_{HB}$  and  $N_{BPX}$  be the ‘nonconforming’ preconditioners given by (2.5). Then there exist constants  $0 < \gamma_{HB} \leq \Gamma_{HB}$  and  $0 < \gamma_{BPX} \leq \Gamma_{BPX}$  depending only on  $\alpha_i, b_i, 0 \leq i \leq 1$ , from (1.2) and on the local geometry of  $\mathcal{T}_0$  such that for all  $v \in CR_{1,0}(\Omega; \mathcal{T}_j)$*

$$\begin{aligned} \frac{\gamma_{HB}}{(j+2)^2} a_{CR}(v, v) &\leq a_{CR}(N_{HB}^{-1} A_{CR} v, v) \leq \Gamma_{HB} a_{CR}(v, v), \\ \gamma_{BPX} a_{CR}(v, v) &\leq a_{CR}(N_{BPX}^{-1} A_L v, v) \leq \Gamma_{BPX} a_{CR}(v, v) \end{aligned} \quad (2.9)$$

where  $A_{CR} : CR_{1,0}(\Omega; \mathcal{T}_j) \longrightarrow CR_{1,0}(\Omega; \mathcal{T}_j)$  is the operator associated with the bilinear form  $a_{CR}(\cdot, \cdot)$ .

**Proof:** We apply Lemma 2.2 with  $S = CR_{1,0}(\Omega; \mathcal{T}_j)$ ,  $V = S_{1,0}(\Omega; \mathcal{T}_{j+1})$ ,  $a_S = a_{CR}$ ,  $a_V = a$  and  $R = I_S, T = P_{CR}$ . Obviously,  $I_S P_{CR} v = v, v \in CR_{1,0}(\Omega; \mathcal{T}_j)$ , so that (2.7 a) is satisfied. Moreover, from Lemma 2.1 it follows readily that (2.7 b) holds true with  $c_0 = \Gamma_{CR}^{-1}$ . Finally, as far as (2.7 c) is concerned, for  $v \in S_{1,0}(\Omega; \mathcal{T}_{j+1})$  we get in view of (1.2), (1.4) and (1.7)

$$\begin{aligned} a_{CR}(I_S v, I_S v) &\leq \alpha_1 C_1 \sum_{T \in \mathcal{T}_j} \sum_{\substack{i,j=1 \\ i < j}}^3 (I_S v(m_i) - I_S v(m_j))^2 + b_1 C_0 \sum_{T \in \mathcal{T}_j} h_T^2 \sum_{i=1}^3 (I_S v(m_i))^2 \\ &= \alpha_1 C_1 \sum_{T \in \mathcal{T}_j} \sum_{\substack{i,j=1 \\ i < j}}^3 (v(m_i) - v(m_j))^2 + b_1 C_0 \sum_{T \in \mathcal{T}_j} h_T^2 \sum_{i=1}^3 (v(m_i))^2 \\ &\leq \alpha_1 C_1 \sum_{T \in \mathcal{T}_{j+1}} \sum_{\substack{i,j=1 \\ i < j}}^3 (v(p_i) - v(p_j))^2 + b_1 C_0 \sum_{T \in \mathcal{T}_{j+1}} h_T^2 \sum_{i=1}^3 (v(p_i))^2 \\ &\leq \alpha_1 c_1^{-1} C_1 |v|_{1;\Omega}^2 + b_1 c_0^{-1} C_0 \|v\|_{0;\Omega}^2 \leq \Gamma_S a(v, v) \end{aligned}$$

where  $\Gamma_S := \frac{1}{\alpha_0} \left( \frac{\alpha_1 C_1}{c_1} + \frac{b_1 C_0 C_P}{c_0} \right)$ . Now, Lemma 2.2 implies

$$\Gamma_{CR}^{-1} a_{CR}(v, v) \leq a_{CR}(I_S A_L^{-1} I_S^* A_{CR} v, v) \leq \Gamma_S a_{CR}(v, v), \quad v \in CR_{1,0}(\Omega; \mathcal{T}_j).$$

The assertion then follows from (2.6) with the constants given by  $\gamma_{HB} := \Gamma_{CR}^{-1} \lambda_{HB}, \gamma_{BPX} := \Gamma_{CR}^{-1} \lambda_{BPX}$  and  $\Gamma_{HB} := \Gamma_S \Lambda_{HB}, \Gamma_{BPX} := \Gamma_S \Lambda_{BPX}$  □

### 3. ERROR ESTIMATOR BASED ON LOCAL SUBPROBLEMS

Reliable and efficient a posteriori error estimators are an indispensable tool for efficient adaptive algorithms. We refer to the pioneering work done by Babuška and Rheinboldt [1, 2] and the recent survey articles by Bornemann et al. [7] and Verfürth [32, 33]. In this section we will focus on an element-oriented error estimator which is based on the solution of local subproblems. In the standard conforming setting this kind of error estimator is due to Bank and Weiser [5]. It relies on a defect correction with respect to the higher order ansatz space of continuous, piecewise quadratics and an appropriate localization based on

a hierarchical two-level splitting. However, in contrast to the standard conforming setting we have to take into account the discontinuity of the nonconforming approximation. This will be done by means of an additional error term involving an appropriate quasi-interpolation operator. It turns out that the estimator can be computed elementwise by the solution of three scalar equations representing a localized defect correction problem and by the evaluation of that quasi-interpolant (cf. [18], [34] and [35]).

In the sequel, we will need the jump  $[v]_J$  and the average  $[v]_A$  of a function  $v$  along an edge of the triangulation. Denoting by  $e$  the common edge of two adjacent elements  $T_{in}$  and  $T_{ex}$  and by  $\mathbf{n}_e$  the unit normal on  $e$  directed towards the interior of  $T_{ex}$ , we define

$$\begin{aligned} [v]_J|_e &:= (v|_{T_{in}} - v|_{T_{ex}})|_e, \\ [v]_A|_e &:= \frac{1}{2}(v|_{T_{in}} + v|_{T_{ex}})|_e. \end{aligned}$$

Moreover, if  $e \subset \partial T_{in} \cap \Gamma$ , we set

$$[v]_J|_e := (v|_{T_{in}})|_e, \quad [v]_A|_e := \frac{1}{2}(v|_{T_{in}})|_e.$$

Throughout the rest of this section we assume that the solution  $u$  of (1.3) lives in  $H^2(\Omega) \cap H_0^1(\Omega)$  and satisfies  $[\mathbf{n}_e \cdot a \nabla u]_J|_e = 0$ ,  $e \in \mathcal{E}_j^0$ .

The construction of the error estimator is based on the following saturation assumption

$$\| \| u - u_Q \| \|_j + \left( \sum_{e \in \mathcal{E}_j} \int_e [\mathbf{n}_e \cdot a \nabla (u - u_Q)]_A^2 d\sigma \right)^{1/2} \leq \beta \| \| u - u_j \| \|_j, \quad 0 < \beta < 1, \quad (3.1)$$

where  $u_Q$  stands for the continuous, piecewise quadratic finite element approximation of (1.3). This saturation assumption is supported by well known a priori error estimates. In particular, if  $u \in H^3(\Omega)$  the conforming finite element solution  $u_Q$  does provide an approximation of  $u$  of order  $O(h^2)$  whereas the nonconforming solution  $u_j$  approximates  $u$  only of order  $O(h)$  (cf. [12]).

In a first step, we consider the linear functional  $\hat{F} : S_{2,0}^{-1}(\Omega; \mathcal{T}_j) \longrightarrow \mathbb{R}$ , defined as

$$\hat{F}(v) := \sum_{T \in \mathcal{T}_j} \int_T (f - L(\hat{u}_j)) v dx - \sum_{e \in \mathcal{E}_j} \int_e [\mathbf{n}_e \cdot a \nabla \hat{u}_j]_J [v]_A d\sigma,$$

where  $\hat{u}_j$  stands for the nonconforming approximation obtained by the iterative solution process as described in section 2 and  $S_{2,0}^{-1}(\Omega; \mathcal{T}_j)$  denotes the space of piecewise quadratic functions vanishing on the boundary  $\Gamma$ .

Since  $\hat{F}$  does not take into account the discontinuity of  $\hat{u}_j$ , we introduce a modified linear functional

$$F(v) := \hat{F}(v - P_L v) + a_{cR} (P_S \hat{u}_j - \hat{u}_j, v)$$

where  $P_L$  and  $P_S$  are appropriately defined operators.

In particular,  $P_L : S_{2,0}^{-1}(\Omega; \mathcal{T}_j) \longrightarrow S_{1,0}^{-1}(\Omega; \mathcal{T}_j)$  is given locally as the Lagrangian interpolation operator

$$P_L v|_T := \sum_{i=1}^3 v|_T(p_i) \psi_{i,T}, \quad v \in S_{2,0}^{-1}(\Omega; \mathcal{T}_j)$$

where  $S_{1,0}^{-1}(\Omega; \mathcal{T}_j)$  is the space of piecewise linear ansatz functions vanishing on the boundary  $\Gamma$  and  $\psi_{i,T}$ ,  $1 \leq i \leq 3$  stand for the local nodal basis functions of  $P_1(T)$ . Obviously, the operator  $P_L$  has the following three properties:

(i) There exists a positive constant  $\gamma_L$  independent of the refinement level  $j$  such that

$$\| \| P_L v_j \| \|_j \leq \gamma_L \| \| v_j \| \|_j, \quad v_j \in S_{2,0}^{-1}(\Omega; \mathcal{T}_j);$$

(ii)  $P_L v_j \in C(\Omega)$  for  $v_j \in S_{2,0}^{-1}(\Omega; \mathcal{T}_j) \cap C(\Omega)$ ;

(iii)  $P_L v_j = v_j$  for  $v_j \in S_{1,0}^{-1}(\Omega; \mathcal{T}_j)$ .

Due to (i), (ii) and (iii) we obtain

$$a_{CR}(v - P_L v, w) \leq \eta^2 \| \| v - P_L v \| \|_j \| \| w \| \|_j, \quad v \in S_{2,0}^{-1}(\Omega; \mathcal{T}_j), w \in S_{1,0}^{-1}(\Omega; \mathcal{T}_j) \quad (3.2)$$

where  $\eta^2 := \frac{\sqrt{\gamma_L^2 - 1}}{\gamma_L} < 1$ . For a detailed proof see [18].

On the other hand, the operator  $P_S : CR_{1,0}(\Omega; \mathcal{T}_j) \rightarrow S_{1,0}(\Omega; \mathcal{T}_j)$  will serve as a measure for the discontinuity of the nonconforming finite element functions. For this purpose we choose the quasi-interpolant as proposed by Oswald in [27].

$$(P_S v)(p) := \begin{cases} 0, & p \in \mathcal{N}_j^\Gamma \\ \frac{1}{\nu_p} \sum_{\nu=1}^{\nu_p} v|_{T_l}(p), & p \in \mathcal{N}_j^0 \end{cases} \quad (3.3)$$

where  $\nu_p$  is the number of triangles  $T_l \in \mathcal{T}_j$  containing  $p$  as a vertex. It is easy to see that  $P_S v = v$  if and only if  $v$  is continuous and satisfies the homogeneous Dirichlet boundary conditions.

Now, if we define  $e \in S_{2,0}^{-1}(\Omega; \mathcal{T}_j)$  as the solution of the following variational problem

$$a_{CR}(e, v) = F(v), \quad v \in S_{2,0}^{-1}(\Omega; \mathcal{T}_j),$$

$e$  gives sharp lower and upper bounds for the total error  $u - \hat{u}_j$  provided the iteration error  $\hat{u}_j - u_j$  is small enough. We remark that, if  $b|_T \equiv 0$  on an interior triangle  $T \in \mathcal{T}_j$ , then  $e|_T$  is not uniquely determined. To obtain uniqueness we require that  $e|_T$  satisfies

$$\int_T e \, dx = \int_T (P_S \hat{u}_j - \hat{u}_j) \, dx. \quad (3.4)$$

It is easy to see that  $e$  can be calculated locally as the solution of an at most  $6 \times 6$  linear system:

$$a_{CR}|_T(e, v) = \hat{F}_T(v - P_L v) + a_{CR}|_T(P_S \hat{u}_j - \hat{u}_j, v), \quad v \in \overline{P}_2(T),$$

where  $\overline{P}_2(T) := \{v \in P_2(T) \mid v|_{\partial\Omega \cap \partial T} = 0\}$ . Again, we require (3.4) in case  $b|_T \equiv 0$ ,  $T \in \mathcal{T}_j \cap \Omega$ .

The definition of the local functional  $\hat{F}_T$ ,  $T \in \mathcal{T}_j$ ,

$$\hat{F}_T(v) := (f, v)_{0;T} - a_{CR}|_T(\hat{u}_j, v) + \sum_{\substack{e \in \mathcal{E}_j \\ e \subset \partial T}} \int_e [\mathbf{n}_e \cdot a \nabla \hat{u}_j]_A v|_T \, d\sigma, \quad v \in S_{2,0}^{-1}(\Omega; \mathcal{T}_j)$$

is consistent with the global definition of  $\hat{F}(\cdot)$  in the sense that  $\hat{F}(v) = \sum_{T \in \mathcal{T}_j} \hat{F}_T(v)$ ,  $v \in S_{2,0}^{-1}(\Omega; \mathcal{T}_j)$ .

**Lemma 3.1.** *Under the saturation assumption (3.1) there hold*

$$\begin{aligned} \| \| u - \hat{u}_j \| \|_j &\leq C_l (\| \| e \| \|_j + \Gamma_l \| \| \hat{u}_j - u_j \| \|_j), \\ \| \| u - \hat{u}_j \| \|_j &\geq c_l (\| \| e \| \|_j - \gamma_l \| \| \hat{u}_j - u_j \| \|_j) \end{aligned} \quad (3.5)$$



where  $c_l, C_l$  and  $\gamma_l, \Gamma_l$  are positive constants independent of the refinement level  $j$ .

**Proof:** cf. [18]. □

Lemma 3.1 states that  $e$  provides sharp lower and upper bounds for the energy norm of the total error if the iteration error is small enough. But  $e$  is only of academic interest and has no practical importance, because the computational amount is too expensive. The rest of this section is devoted to establish an error estimator which requires less computational work. For this purpose, we first consider the elliptic projection of the so-called continuous part of  $e|_T$  onto the three-dimensional subspace of quadratic bubble functions associated with the midpoints of the edges. In a second step, we neglect the coupling between the bubbles and obtain three scalar equations to solve.

We define  $\hat{e}$  as the solution of

$$a_{CR}(\hat{e}, v) = \hat{F}(v - P_L v), \quad v \in S_{2,0}^{-1}(\Omega; \mathcal{T}_j). \quad (3.6)$$

and

$$\int_T \hat{e} dx = 0,$$

if  $b|_T \equiv 0$  on an interior element  $T \in \mathcal{T}_j$ . Then, it is easy to see that  $\hat{e} = e + \hat{u}_j - P_S \hat{u}_j$  and

$$\|e\|_j^2 = \|\hat{e}\|_j^2 + \|\hat{u}_j - P_S \hat{u}_j\|_j^2. \quad (3.7)$$

Now, we will concentrate on the construction of an adequate replacement of  $\hat{e}$  which can be obtained by the solution of scalar equations. We decompose  $S_{2,0}^{-1}(\Omega; \mathcal{T}_j)$  into the direct sum of  $S_{1,0}^{-1}(\Omega; \mathcal{T}_j)$  and the hierarchical surplus  $\tilde{S}_{2,0}^{-1}(\Omega; \mathcal{T}_j) := \{v \in S_{2,0}^{-1}(\Omega; \mathcal{T}_j) \mid P_L v = 0\}$ . Based on this splitting, we obtain  $\tilde{e} \in \tilde{S}_{2,0}^{-1}(\Omega; \mathcal{T}_j)$  as the uniquely defined solution of

$$a_{CR}|_T(\tilde{e}, v) = \hat{F}_T(v), \quad v \in \tilde{S}_{2,0}^{-1}(\Omega; \mathcal{T}_j). \quad (3.8)$$

The following lemma shows the equivalence of  $\|\hat{e}\|_j$  and  $\|\tilde{e}\|_j$ .

**Lemma 3.2.** *Let  $\hat{e}, \tilde{e}$  be given by (3.6) and (3.8), respectively. Then there holds*

$$\|\tilde{e}\|_j \leq \|\hat{e}\|_j \leq \frac{1}{(1 - \eta^2)^{1/2}} \|\tilde{e}\|_j.$$

**Proof:** In view of

$$a_{CR}(\tilde{e}, v) = \hat{F}(v) = \hat{F}(v - P_L v) = a_{CR}(\hat{e}, v), \quad v \in \tilde{S}_{2,0}^{-1}(\Omega; \mathcal{T}_j)$$

it follows that  $\tilde{e}$  is the elliptic projection of  $\hat{e}$  onto  $\tilde{S}_{2,0}^{-1}(\Omega; \mathcal{T}_j)$  whence  $\|\tilde{e}\|_j \leq \|\hat{e}\|_j$ . Hence, only the second inequality remains to be shown. For that purpose we decompose  $\hat{e}$  according to  $\hat{e} = (\hat{e} - P_L \hat{e}) + P_L \hat{e}$ . By means of (3.6) we obtain

$$a_{CR}(\hat{e}, P_L \hat{e}) = 0,$$

yielding  $a_{CR}(P_L \hat{e}, P_L \hat{e}) = -a_{CR}(P_L \hat{e}, \hat{e} - P_L \hat{e})$ . Using (3.2) it follows that

$$\begin{aligned} \|\hat{e}\|_j^2 &= a_{CR}(\hat{e} - P_L \hat{e}, \hat{e} - P_L \hat{e}) + a_{CR}(\hat{e} - P_L \hat{e}, P_L \hat{e}) \\ &\geq \|\hat{e} - P_L \hat{e}\|_j (\|\hat{e} - P_L \hat{e}\|_j - \eta^2 \|P_L \hat{e}\|_j) \\ &\geq (1 - \eta^2) \|\hat{e} - P_L \hat{e}\|_j^2. \end{aligned}$$

Altogether, we get

$$\begin{aligned} \|\hat{e}\|_j^2 &= a_{CR}(\hat{e}, \hat{e} - P_L \hat{e}) = a_{CR}(\tilde{e}, \hat{e} - P_L \hat{e}) \\ &\leq \frac{1}{(1 - \eta^2)^{1/2}} \|\hat{e}\|_j \|\tilde{e}\|_j. \end{aligned}$$

□

The local  $3 \times 3$  stiffness matrices of the variational problem (3.8) are spectrally equivalent to their diagonal matrices. Note, that the constants are independent of the refinement level and only depend on  $\alpha_i, b_i, 0 \leq i \leq 1$ , in (1.2) and the local geometry of the initial triangulation. We define  $\phi_T^i := \varpi_i \phi_{e_i}|_T, 1 \leq i \leq 3$ , where  $\varpi_i \in \mathbb{R}$  is given as

$$\varpi_i := \frac{\hat{F}_T(\phi_{e_i})}{a_{CR}|_T(\phi_{e_i}, \phi_{e_i})}$$

and  $\phi_{e_i}$  denote the quadratic bubble functions associated with the edges  $e_i, 1 \leq i \leq 3$ . Due to the spectral equivalence we obtain

$$c \|\tilde{e}\|_{j;T} \leq \sum_{i=1}^3 \|\phi_T^i\|_{j;T} \leq C \|\tilde{e}\|_{j;T}, \quad T \in \mathcal{T}_j, \quad (3.9)$$

with some constants  $0 < c \leq C$  independent of the refinement level  $j$ . In view of the preceding results we are led to the following error estimator  $e^l$ :

$$\begin{aligned} (e^l)^2 &:= \sum_{T \in \mathcal{T}_j} (e_T^l)^2, \\ (e_T^l)^2 &:= \sum_{i=1}^3 \|\phi_T^i\|_{j;T}^2 + \|\hat{u}_j - P_S \hat{u}_j\|_{j;T}^2. \end{aligned}$$

The following theorem states that  $e^l$  is an efficient and reliable error estimator, if the iteration error  $u_j - \hat{u}_j$  is small enough.

**Theorem 3.1.** *Under the assumption (3.1) there exist positive constants  $\hat{c}_l, \hat{C}_l$  and  $\hat{\gamma}_l, \hat{\Gamma}_l$  independent of the refinement level  $j$  such that*

$$\begin{aligned} \|u - \hat{u}_j\|_j &\leq \hat{C}_l (e^l + \hat{\Gamma}_l \|u_j - \hat{u}_j\|_j), \\ \|u - \hat{u}_j\|_j &\geq \hat{c}_l (e^l - \hat{\gamma}_l \|u_j - \hat{u}_j\|_j). \end{aligned} \quad (3.10)$$

**Proof:** The theorem is a direct consequence of Lemma 3.1, Lemma 3.2, the orthogonality relation (3.7) and the equivalence (3.9). □

The computational amount for  $e^l$  is significantly less than that for  $\|e\|_j$ . We only have to solve three scalar equations per element and to take into account the discontinuity of  $\hat{u}_j$  which is taken care of by the additional term  $\|P_S \hat{u}_j - \hat{u}_j\|_j$ .

#### 4. NUMERICAL RESULTS

In this section, we will illustrate the adaptive refinement process and the performance of both the multilevel preconditioners and the error estimator by numerical results for two selected test problems. Further, we will document the application of the adaptive algorithm in semiconductor device simulation and in reactor kinetics.

As test examples we have chosen the following model problems from [21] where the solutions exhibit singularities of different order.

*Problem 1a* (reentrant corner). We consider the Laplace equation on the L-shaped domain  $\Omega = (-1, 1) \times (-1, 1) \setminus (0, 1) \times (-1, 0)$ . In polar coordinates the solution is given by  $u = r^{2/3} \sin\left(\frac{2\theta}{3}\right)$ .

*Problem 1b* (slit domain). The Laplace equation is considered on a hexagon with a slit along the line  $y = 0$  and  $0 < x < 1$  (cf. Figure 4.2). In polar coordinates the solution is given by  $u = r^{1/4} \sin\left(\frac{\theta}{4}\right)$ .

Starting from the initial coarse triangulations as shown in Figures 4.1, 4.2, the discretized problems have been solved by the adaptive multilevel algorithm as described in the preceding sections. In particular, on level  $k + 1$ ,  $0 \leq k \leq j - 1$ , the startiterate  $\hat{u}_{k+1}^0$  is obtained from the computed solution  $\hat{u}_k$  on level  $k$  by means of the prolongation  $\hat{u}_{k+1}^0(m) := \frac{1}{2}(\hat{u}_k|_{T_1}(m) + \hat{u}_k|_{T_2}(m))$  where  $m \in \mathcal{M}_{k+1}^0$  is the midpoint of the common edge of two adjacent triangles  $T_1, T_2 \in \mathcal{T}_{k+1}$ . The iteration on level  $k + 1$  has been stopped when the estimated iteration error  $\varepsilon_{k+1}$  satisfied  $\varepsilon_{k+1}^2 \leq \mu \varepsilon_k^2 \frac{N_k}{N_{k+1}}$  where  $\varepsilon_k$  denotes the estimated error on level  $k$ ,  $N_k$  the number of nodes on level  $k$  and  $\mu$  is a safety factor which has been chosen as  $\mu = 1.E - 2$ . For the adaptive refinement process we have used the meanwhile standard technique due to Bank et al. [4] with a slight modification. Instead of the simple mean-value strategy we have taken into account the area of the triangles which results in some kind of an extrapolation strategy. A triangle  $T \in \mathcal{T}_k$  has been marked for refinement if

$$\frac{(e_T^l)^2}{|T|} \geq \frac{\tau}{|\Omega|} \sum_{T \in \mathcal{T}_k} (e_T^l)^2$$

where  $|T|$ ,  $|\Omega|$  stand for the area of  $T$  and  $\Omega$ , respectively, and  $\tau = 0.95$ . Finally, the

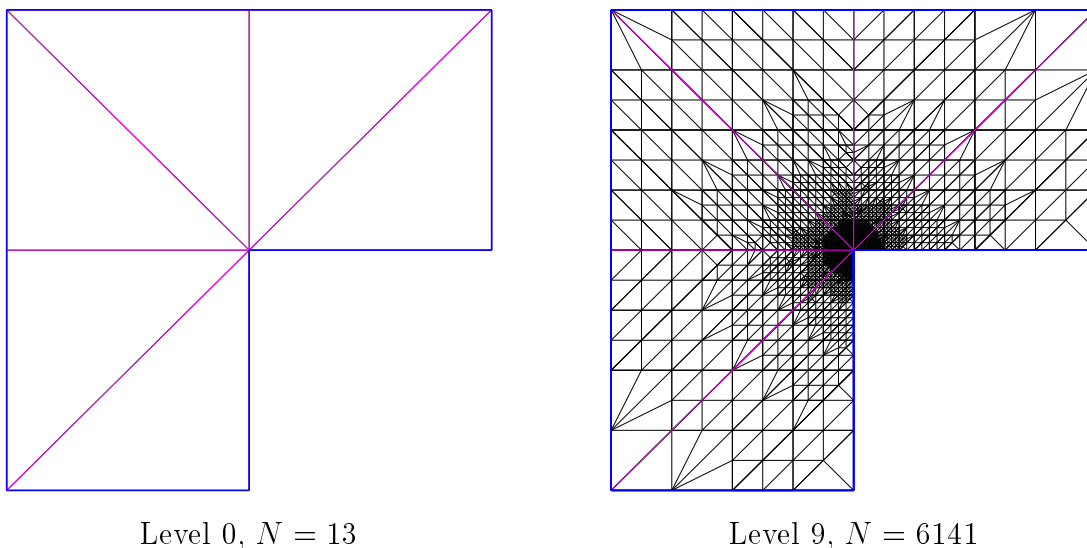


Figure 4.1: Initial triangulation  $\mathcal{T}_0$  and final triangulation  $\mathcal{T}_9$  (Problem 1a)

refinement process has been stopped when the ratio of the estimated error and the norm of the iterative approximation was less than the required accuracy  $TOL$  times a safety factor  $\alpha$ . In particular, we have chosen  $TOL = 2.75E - 2$  (Problem 1a),  $TOL = 2.75E - 1$  (Problem 1b) and  $\alpha = 0.98$ .

Figure 4.1 and Figure 4.2 represent the initial and final triangulations for Problem 1a, 1b. We observe a pronounced refinement in the vicinity of the reentrant corner (Problem 1a) and the origin (Problem 1b).

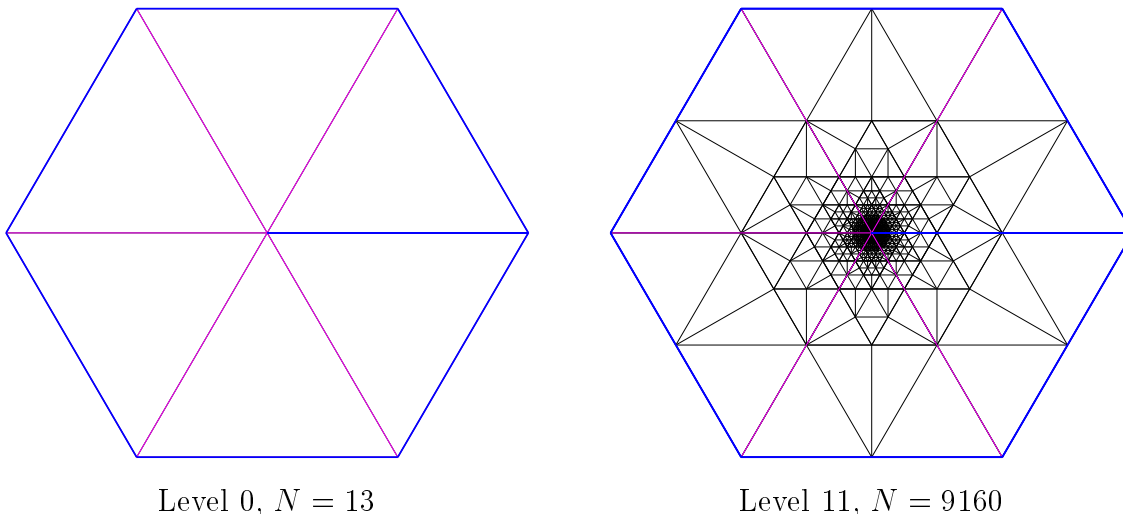


Figure 4.2: Initial triangulation  $\mathcal{T}_0$  and final triangulation  $\mathcal{T}_{11}$  (Problem 1b)

Figure 4.3 and 4.4 display the number of multilevel preconditioned cg-iterations as a function of the total number of nodes thus illustrating the performance of the preconditioners.

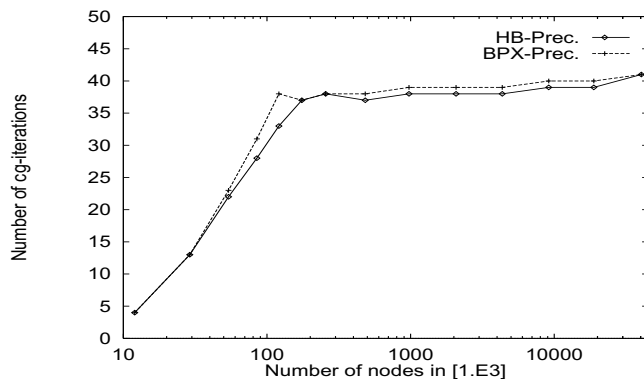


Figure 4.3: Performance of the preconditioners (Problem 1a)

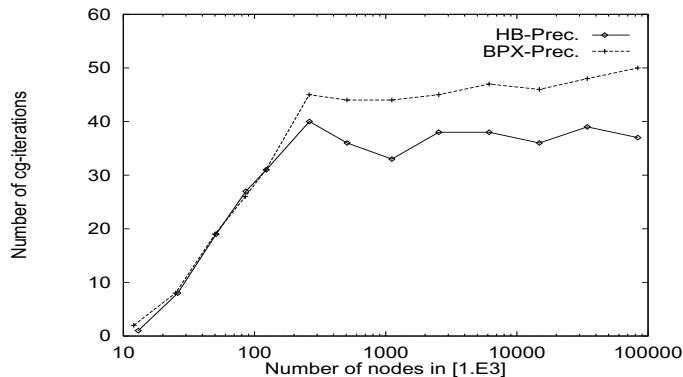


Figure 4.4: Performance of the preconditioners (Problem 1b)

The results for the BPX-type preconditioner are in accordance with the theoretically predicted  $O(1)$  behavior (cf. Theorem 2.1). On the other hand, for both problems the hierarchical basis type preconditioner exhibits the same asymptotic behavior which is better than the theoretically expected quadratic growths in the number of refinement levels.

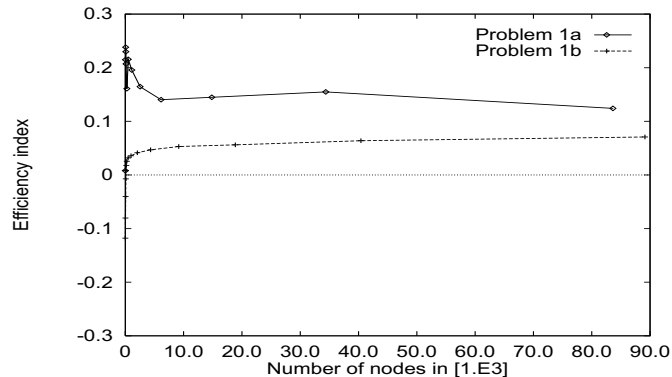


Figure 4.5: Behavior of the efficiency index

Figure 4.5 shows the efficiency index  $\eta := \frac{\epsilon_{est}}{\epsilon_{true}} - 1$  as a function of the total number of nodal points where  $\epsilon_{est}$  and  $\epsilon_{true}$  stand for the estimated and true error, respectively. In both cases we observe a slight overestimation of the true error. We also note that the error estimator is not asymptotically exact, i.e., the efficiency index does not converge to zero as the total number of nodes goes to infinity.

The next example represents a slightly simplified benchmark problem from the International Atomic Energy Authority concerning the computation of the neutron fluxes in a light water reactor based on the two-group neutron diffusion equations.

$$\begin{aligned}
 -\nabla(D_1 \nabla \phi_1) + (\Sigma_{a1} + \Sigma_{12})\phi_1 &= \frac{1}{\lambda} \nu \chi_1 (\Sigma_{f1} \phi_1 + \Sigma_{f2} \phi_2), \\
 -\nabla(D_2 \nabla \phi_2) + \Sigma_{a2} \phi_2 - \Sigma_{12} \phi_1 &= \frac{1}{\lambda} \nu \chi_2 (\Sigma_{f1} \phi_1 + \Sigma_{f2} \phi_2).
 \end{aligned}
 \tag{4.1}$$

Here  $\phi_i$  denotes the neutron flux of the energy group  $i$  and  $D_i$ ,  $1 \leq i \leq 2$ , are the associated diffusion coefficients.  $\lambda$  stands for the critical constant of the reactor (generalized eigenvalue),  $\nu$  is the number of prompt neutrons and  $\chi_i$ ,  $\Sigma_{ai}$ ,  $\Sigma_{fi}$ ,  $\Sigma_{12}$ ,  $1 \leq i \leq 2$ , represent the fission spectrum of prompt neutrons and the absorption, fission and scattering cross sections which are physical parameters. Note that we do not consider external sources and scattering from the energy group 2 (slow neutrons) to group 1 (fast neutrons).

	$D_1$	$D_2$	$\Sigma_{a1}$	$\Sigma_{a2}$	$\nu \Sigma_{f1}$	$\nu \Sigma_{f2}$	$\chi_1$	$\chi_2$	$\Sigma_{12}$
Region 1	2.0	0.300	0.0	0.010	0.0	0.0	1.0	0.0	0.04
Region 2	1.5	0.400	0.01	0.085	0.0	0.135	1.0	0.0	0.02
Region 3	1.5	0.209	0.01	0.400	0.0	0.135	1.0	0.0	0.02

Table 4.1: Parameters of the benchmark problem

For symmetry reasons, the computational domain can be chosen as the upper right quarter of the cross section of the reactor core which is shown in Figure 4.6 along with the associated boundary conditions. We consider two differently enriched regions (region 2,

3) and the light water reflector (region 1). The physical parameters for the three regions are given in Table 4.1. For more details we refer to [30], [31].

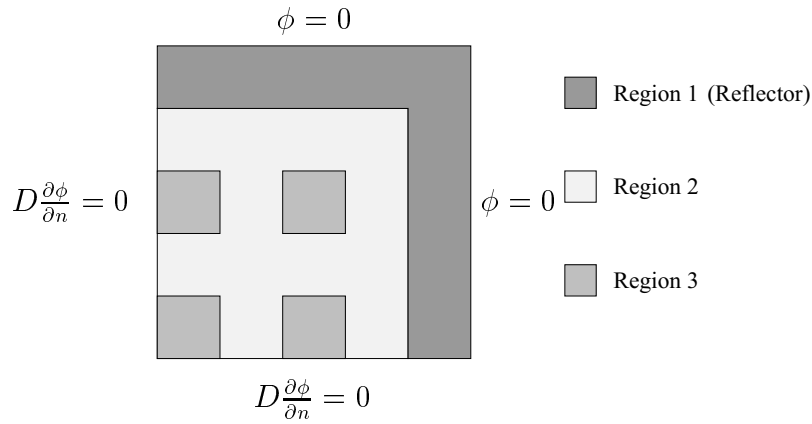


Figure 4.6: Geometry of the benchmark problem

We have discretized (4.1) by a mixed finite element approach based on the lowest order Raviart-Thomas elements. More specifically, we have applied the technique of mixed hybridization leading to an equivalent nonconforming discretization that has been

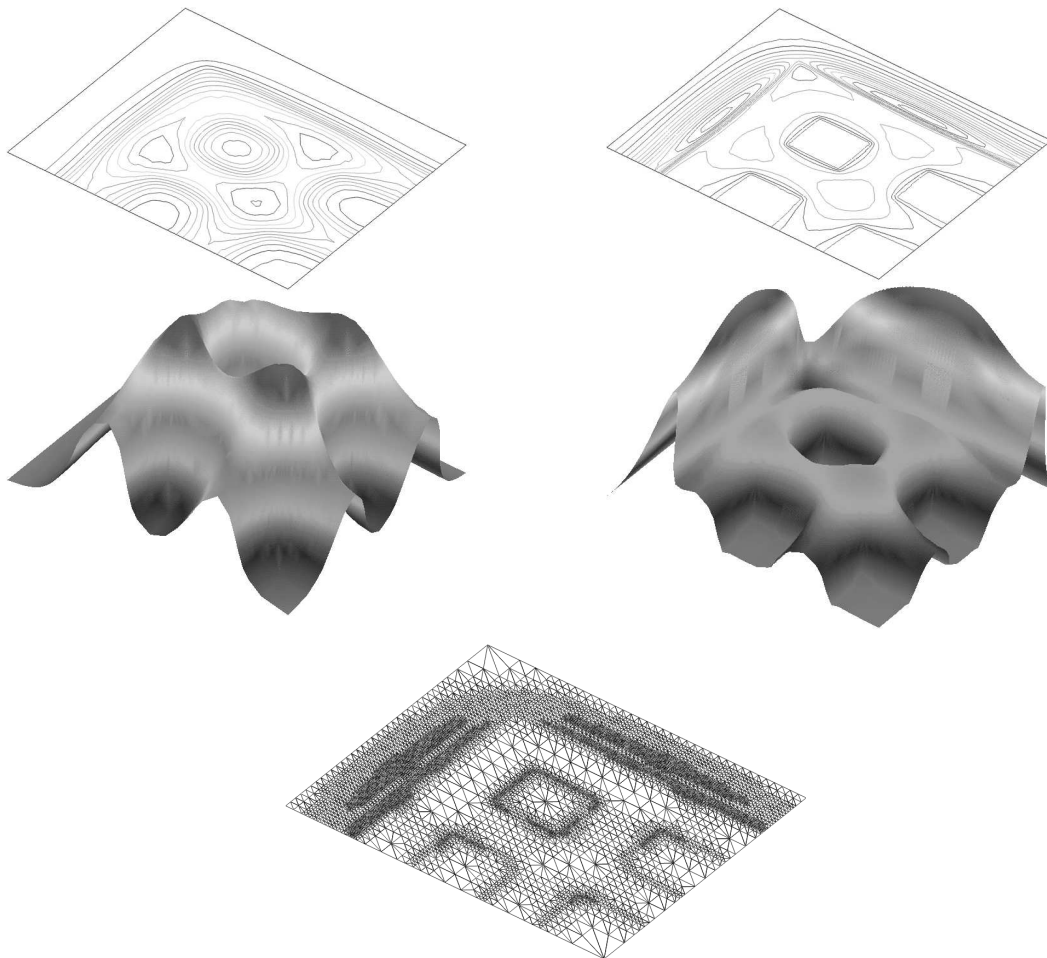


Figure 4.7: Neutron flux of energy group 1 (left) and 2 (right)

solved by the multilevel algorithm described in section 2. In particular, we have used an outer/inner iterative method featuring a block Gauss-Seidel scheme as the outer iteration and the multilevel preconditioned cg-iteration with the BPX-type preconditioner of section 2 as the inner iteration. The adaptive refinement of the triangulations has been realized by an error estimator for the  $L^2$ -norm of the neutron flux of the energy group 2 (for details about that error estimator cf. e.g. [19]).

Figure 4.7 contains the adaptively generated grid (bottom) and a visualization of the neutron fluxes of both energy groups along with a graphical representation of the corresponding contour lines (top). We observe an accurate resolution of both the interfaces between the different regions and of the layer within the reflector zone.

As another example of practical relevance we consider the numerical simulation of a reverse biased  $pn$ -junction which is a specific microelectronic device that is used for blocking purposes in technical applications.

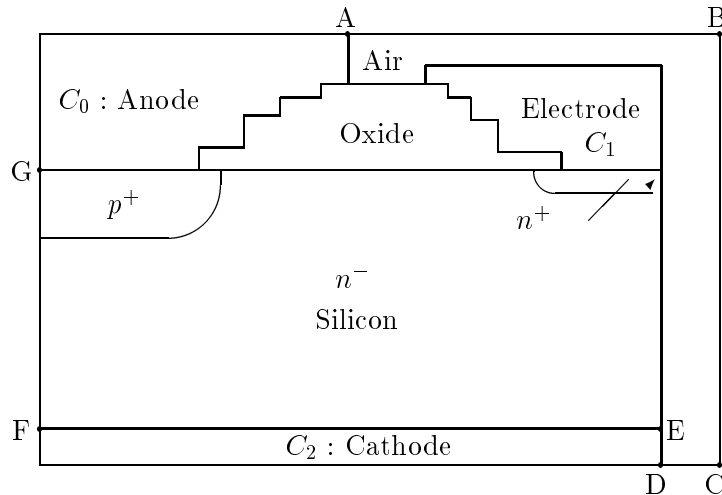


Figure 4.8: Scheme of a planar  $pn$ -junction

Figure 4.8 shows the simplified geometry of the device. In active mode a constant negative voltage is applied to the anode whereas the other contacts (stop-electrode and cathode) are kept voltage-free. At the  $pn$ -junction the electric field causes the electrons and holes to move towards the  $n$ - and  $p$ -region, respectively. In this way, a depletion area of ideally no carrier concentrations is created in a vicinity of the  $pn$ -junction so that there is no flow of a current. The blocking ability of the device can be influenced by multistep field plates and the placement of the stop-electrode (cf. e.g. [17]).

The problem can be formulated as a free boundary problem for a second order elliptic partial differential equation

$$-\operatorname{div}(\epsilon \nabla \psi) = qD(1 - \delta_{\psi,0} - \delta_{\psi,-\psi_0}) \quad (4.2)$$

where  $\psi$  is the potential of the electric field,  $\epsilon$  the electric permittivity,  $q$  the elementary charge,  $D$  the dopand profile,  $-\psi_0$  the applied voltage at the anode and  $\delta_{x,y}$  stands for the Kronecker symbol. The boundary conditions are of Dirichlet type at the contacts and of homogeneous Neumann type elsewhere. The free boundary is given by the interfaces between the depletion area and the  $p$ - and  $n$ -region, respectively. In contrast to the approach used in [20] we have tackled the problem by a front-tracking method based on the nonconforming P1 approximation of (4.2). The resulting discretized elliptic boundary

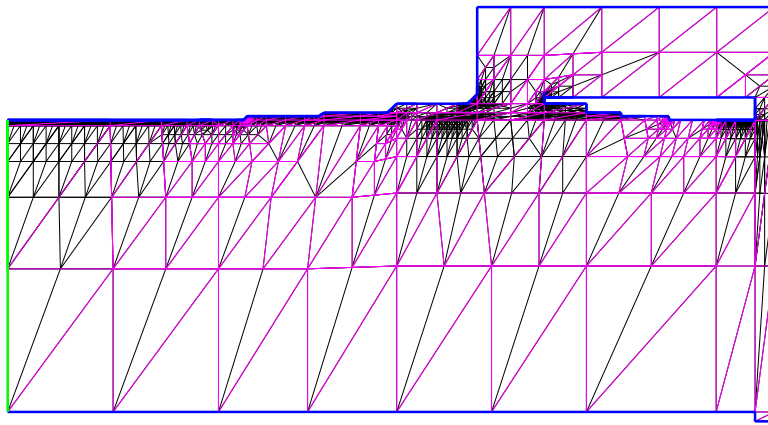


Figure 4.9: Adaptive refined grid on level 6

value problems have been solved by the adaptive multilevel algorithm described in the preceding sections. In particular, we have used the BPX-type multilevel preconditioner.

Figure 4.9 shows the adaptively generated final triangulation featuring a significant local refinement in the vicinity of the multistep field plates and at the interface between the silicon and the oxide where the electric permittivity has a jump discontinuity. Figure 4.10 below displays the distribution of the electric field in the area between the field plates and the stop-electrode as well as the underlying triangulation.

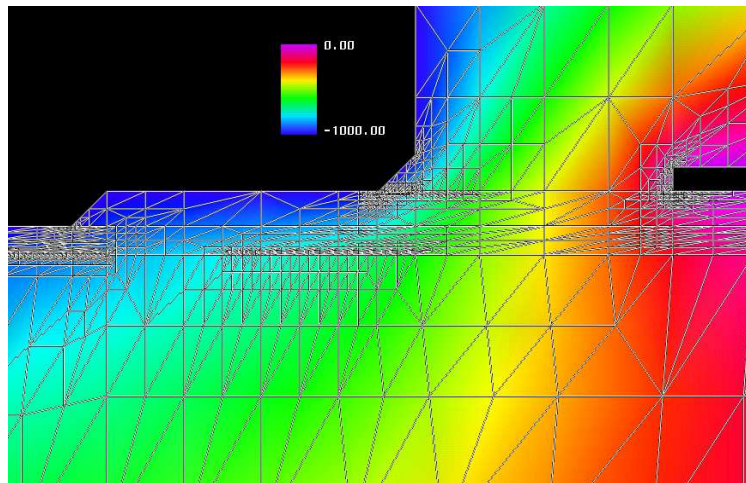


Figure 4.10: Zoom of the distribution of the electric field

## References

- [1] I. Babuška and W.C. Rheinboldt, *Error estimates for adaptive finite element computations*. SIAM J. Numer. Anal. 15, 736-754 (1978)
- [2] I. Babuška and W.C. Rheinboldt, *A posteriori error estimates for the finite element method*. Int. J. Numer. Methods Eng. 12, 1597-1615 (1978)
- [3] R.E. Bank, *PLTMG - A Software Package for Solving Elliptic Partial Differential Equations. User's Guide 6.0*. SIAM, Philadelphia, 1990
- [4] R.E. Bank, A.H. Sherman and A. Weiser, *Refinement algorithm and data structures for regular local mesh refinement*. In: Scientific Computing, R. Stepleman et al. (eds.), p. 3-17, IMACS North-Holland, Amsterdam, 1983



- [5] R.E. Bank and A. Weiser, *Some a posteriori error estimators for elliptic partial differential equations*. Math. Comp. 44, 283-301 (1985)
- [6] F. Bornemann, *A Sharpened Condition Number Estimate for the BPX Preconditioner of Elliptic Finite Element Problems on Highly Nonuniform Triangulations*. Konrad-Zuse-Zentrum für Informationstechnik Berlin. Preprint SC 91-9, 1991
- [7] F. Bornemann, B. Erdmann and R. Kornhuber, *A posteriori error estimates for elliptic problems in two and three space dimensions*. Konrad-Zuse-Zentrum für Informationstechnik Berlin. Preprint SC 93-29, 1993
- [8] F. Bornemann and H. Yserentant, *A basic norm equivalence for the theory of multilevel methods*. Numer. Math. 64, 445-476 (1993)
- [9] D. Braess and R. Verfürth, *Multigrid methods for nonconforming finite element methods*. SIAM J. Numer. Anal. 27, No. 4, 979-986 (1990)
- [10] J.H. Bramble, J.E. Pasciak, J. Xu, *Parallel multilevel preconditioners*. Math. Comp. 55, 1-22 (1990)
- [11] S. Brenner, *An optimal-order multigrid method for P1 nonconforming finite elements*. Math. Comp. 53, 1-15 (1989)
- [12] P. Ciarlet, *The finite element method for elliptic problems*. North-Holland, Amsterdam, 1987
- [13] L.C. Cowsar, *Domain decomposition methods for nonconforming finite element spaces of Lagrange-type*. Rice University, Houston. Preprint TR 93-11, 1993
- [14] W. Dahmen and A. Kunoth, *Multilevel preconditioning*. Numer. Math. 63, 315-344 (1992)
- [15] P. Deuffhard, P. Leinen and H. Yserentant, *Concepts of an adaptive hierarchical finite element code*. IMPACT Comput. Sci. Engrg. 1, 3-35 (1989)
- [16] M. Dryja and O.B. Widlund, *Towards a unified theory of domain decomposition algorithms for elliptic problems*. In: Proc. 3rd Int. Symp. on Domain Decomposition Methods for Partial Differential Equations, T.F. Chan et al. (eds.), p. 3-21, SIAM, Philadelphia, 1990
- [17] E. Falck and W. Gerlach *Berechnung der Durchbruchsspannung von planaren pn-Übergängen mit mehrstufigen Feldplatten*. AEÜ 43, 328-334 (1989)
- [18] R.H.W. Hoppe and B. Wohlmuth, *Element-oriented and edge-oriented local error estimators for nonconforming finite element methods*. To appear in  $M^2AN$  Math. Modelling and Numer. Anal.
- [19] R.H.W. Hoppe and B. Wohlmuth, *Efficient Numerical Solution of Mixed Finite Element Discretizations by Adaptive Multilevel Methods*. Apl. Mat. 40, 227-248 (1995)
- [20] R. Kornhuber and R. Roitzsch, *Self Adaptive Computatin of the Breakdown Voltage of Planar pn-Junctions with Multistep Field Plates*. In: Proc. 4th Int. Conf. of Semiconductor Devices and Processes., Fichtner et al. (eds.), p. 535-543, Zürich, 1991
- [21] W.F. Mitchell, *A Comparison of Adaptive Refinement Techniques for Elliptic Problems*. UIUCDCS R-87-1375, University of Illinois at Urbana-Champaign (1987)
- [22] S.V. Nepomnyaschikh, *Fictitious components and subdomain alternating methods*. Sov. J. Numer. Anal. Math. Modelling 5, 53-68 (1990)
- [23] S.V. Nepomnyaschikh, *Decomposition and fictitious domain methods for elliptic boundary value problems*. In: Proc. 5th Int. Symp. on Domain Decomposition Methods for Partial Differential Equation, D.F. Keyes et al. (eds.), p. 62-72, SIAM, Philadelphia, 1992
- [24] P. Oswald, *Two remarks on multilevel preconditioners*. Forsch.-Erg. FSU Jena, Math. /91/1, 1991
- [25] P. Oswald, *On a hierarchical basis multilevel method with nonconforming P1 elements*. Numer. Math. 62, 189-212 (1992)
- [26] P. Oswald, *On discrete norm estimates related to multilevel preconditioner in the finite element methods*. In: Constructive Theory of functions, K.G. Ivanov et al. (eds.), p. 203-214, Bulg. Acad. Sci, Sofia, 1992
- [27] P. Oswald, *On a BPX-preconditioner for P1 elements*. Computing 51, 125-133 (1993)
- [28] P. Oswald, *Multilevel finite element approximation: Theory and Application*. Teubner-Skripten zur Numerik, Teubner, Stuttgart, 1994
- [29] M. Sarkis, *Two-Level Schwarz Methods for Nonconforming Finite Elements and Discontinuous Coefficients*. TR 629, Courant Institute of Mathematical Sciences, New York, 1993
- [30] W. Schmid, *Solution of the Neutron Diffusion Equation*. ZAMM 75 S II, 709-710 (1995)

- [31] W. Schmid and F. Wagner, *Numerical Solution of the Neutron Diffusion Equation - Adaptive Concepts in Time and Space*. to appear in Numerical Treatment of Coupled Systems. In: Proc. of the 11th. GAMM-Seminar. Notes on Numerical Fluid Mechanics, Vol. 51, Kiel, 1995
- [32] R. Verfürth, *A posteriori error estimation and adaptive mesh-refinement techniques*. To appear in J. Comp. Appl. Math.
- [33] R. Verfürth, *A review of a posteriori error estimation and adaptive mesh-refinement techniques*. Manuscript, 1993
- [34] B. Wohlmuth, *Adaptive Multilevel-Finite-Elemente Methoden zur Lösung elliptischer Randwertprobleme*. Ph. Thesis, Technische Universität München (1995)
- [35] B. Wohlmuth and R.H.W. Hoppe, *Multilevel approaches to nonconforming finite element discretizations of linear second order elliptic boundary value problems*. Journal of Computation and Information 4, 73-86 (1994)
- [36] J. Xu, *Iterative methods by space decomposition and subspace correction*. SIAM Rev. 34, 581-613 (1992)
- [37] H. Yserentant, *On the multi-level splitting of finite element spaces*. Numer. Math. 49, 379-412 (1986)
- [38] H. Yserentant, *Old and new convergence proofs for multigrid methods*. Acta Numerica 1, 285-326 (1993)
- [39] X. Zhang, *Multilevel Schwarz methods*. Numer. Math. 63, 521-539 (1992)